Arterial Wall Mechanics in Conscious Dogs

Assessment of Viscous, Inertial, and Elastic Moduli to Characterize Aortic Wall Behavior

Ricardo Luis Armentano, Juan Gabriel Barra, Jaime Levenson, Alain Simon, Ricardo Horacio Pichel

Abstract To evaluate arterial physiopathology, complete arterial wall mechanical characterization is necessary. This study presents a model for determining the elastic response of elastin (σ_E, where σ is stress), collagen (σ_C), and smooth muscle (σ_{SM}) fibers and viscous (σ_η) and inertial (σ_M) aortic wall behaviors. Our work assumes that the total stress developed by the wall to resist stretching is governed by the elastic modulus of elastin fibers (E_E), the elastic modulus of collagen (E_C) affected by the fraction of collagen fibers (f_C) recruited to support wall stress, and the elastic modulus of the maximally contracted vascular smooth muscle (E_{SM}) affected by an activation function (f_A). We constructed the constitutive equation of the aortic wall on the basis of three different hookean materials and two nonlinear functions, f_A and f_C:

$$\sigma=\sigma_E+\sigma_C+\sigma_{SM}+\sigma_\eta+\sigma_M=E_E\cdot(\varepsilon-\varepsilon_{0E})+E_C\cdot f_C\cdot\varepsilon+E_{SM}\cdot f_A\cdot\varepsilon+\eta\cdot\frac{d\varepsilon}{dt}+M\cdot\frac{d^2\varepsilon}{dt^2}$$

where ε is strain and ε_{0E} is strain at zero stress. Stress-strain relations in the control state and during activation of smooth muscle (phenylephrine, 5 $\mu g\cdot kg^{-1}\cdot min^{-1}$ IV) were obtained by transient occlusions of the descending aorta and the inferior vena cava in 15 conscious dogs by using descending thoracic aortic pressure (microtransducer) and diameter (sonomicrometry) measurements. The f_C was not linear with strain, and at the onset of significant collagen participation in the elastic response (break point of the stress-strain relation), 6.02±2.6% collagen fibers were recruited at 23% of stretching of the unstressed diameter. The f_A exhibited a skewed unimodal curve with a maximum level of activation at 28.3±7.9% of stretching. The aortic wall dynamic behavior was modified by activation increasing viscous (η) and inertial (M) moduli from the control to active state (viscous, $3.8\pm1.3\times10^4$ to $7.8\pm1.1\times10^4$ dyne·s·cm^{-2}, $P<.0005$; inertial, 61±42 to 91±23 dyne·s^2·cm^{-2}, $P<.05$). Finally, the purely elastic stress-strain relation was assessed by subtracting the viscous and inertial behaviors. (***Circ Res.* 1995; 76:468-478.**)

Key Words • aortic mechanical properties • constitutive equation • stress-strain relation • collagen recruitment function • vascular smooth muscle activation function

The arterial load can be separated into three components: systemic vascular resistance, total arterial elasticity, and wave reflection.[1] Although arterial resistance exerts the greatest effect on ventricular stroke output, an increase of arterial elasticity might result in less optimal coupling of the heart to the arteries with a concomitant less efficient energy utilization by the left ventricle.[2] In particular, a decrease in compliance might increase systolic blood pressure[3] and create extra cardiac load.[4] An important feature of atherogenesis is the focal smooth muscle cell proliferation accompanied by matrix fiber accumulation. Characterization of the elastic behavior of arterial wall constituents in normal and diseased vessels may provide insight into the mechanical factors that could modulate the morphogenesis of atherosclerotic plaques or contribute to the pathogenesis of medial sclerosis.[5]

The individual elastic behavior of structural constituents of the aortic wall has been assessed in response to vitamin D_3–induced accelerated calcinosis[6] and under chronic converting enzyme inhibition on aortic stiffening induced by renovascular hypertension in conscious dogs.[7] In the first report,[6] the accelerated, severe, experimental calcinosis–induced calcium deposition inside the wall of large arteries was shown to be accompanied by a clear-cut paradoxical reduction in arterial rigidity that was mainly due to functional and structural modification of collagen elasticity. The other report[7] showed that arterial elasticity in hypertensive dogs was probably altered by changes in vascular smooth muscle (VSM) activity induced by angiotensin-mediated renovascular hypertension. Chronic converting enzyme inhibition decreased the aortic stiffness induced by renovascular hypertension, specifically changing the elastic behavior of elastin and smooth muscle fibers.[7]

The individual contribution of elastin and collagen fibers to whole aortic elasticity has been previously assessed in normal and diseased conscious dogs.[8] In that study, the elastic modulus of the whole aortic wall was decomposed into the elastic modulus of elastin fibers (E_E), the elastic modulus of collagen fibers (E_C), and the recruitment of collagen fibers (f_C, the strain recruitment function) supporting wall stress at a given transmural pressure. The elastic contribution of VSM in conscious animals has been recently assessed by using a modified Maxwell model consisting of a contractile element (CE), which behaves as a simple viscous element in the resting muscle and offers no permanent resistance to stretching, an elastic spring (SEC) coupled in series with the CE,

Received July 7, 1994; accepted November 15, 1994.

From the Basic Sciences Research Institute (R.L.A., J.G.B., R.H.P.), Favaloro Foundation, Buenos Aires, Argentina, and the Centre de Médicine Preventive Cardiovasculaire (J.L., A.S.), Hôpital Broussais, Paris, France.

Reprint requests to Ricardo Armentano, EEng, PhD, Basic Sciences Research Institute, Favaloro Foundation, Solís 453, (1078) Buenos Aires, Argentina.

and a parallel elastic component (PEC), which represents the elastic behavior of the aortic wall when the smooth muscle is relaxed or under normal vasomotor tone with negligible elastic effects.[9]

However, viscous and inertial contributions to aortic wall mechanics, evidenced by the hysteresis seen in the stress-strain relation, have not been previously studied.[10-13] Besides, Fung[14] has pointed out the lack (until the present study) of constitutive equations of smooth muscle, which are necessary to analyze the function of different organs, and the urgent need for research to fill this gap.

To our knowledge, no study regarding a complete specification of the mechanical properties of the aortic wall has been reported in conscious animals. The study of the mechanical properties of the aortic wall using conscious animal preparations was pointed out by Dobrin,[15] who stated that constriction of large arteries is not usually seen in anesthetized animals. Moreover, the in vivo characterization is a striking procedure that allows a complete description of the arterial mechanical properties under a conceptual framework destined to evaluate the arterial physiopathology both in clinical and experimental research. A possible reason that this analysis has not been performed in conscious animals could be the difficulty in characterizing the complex structure of the aortic wall, whose constituents have very different mechanical properties that produce nonlinear stress-strain relations when pressure and diameter are examined over a wide range. Moreover, the nonlinearity between stress and strain signals can hinder the quantification of the viscous and inertial moduli in the frequency domain. To solve this problem, it is crucial to develop algorithms in the time domain, where nonlinearity does not cause any difficulties.

The goal of the present study is to give some insight into the complete characterization of the mechanical properties of the aortic wall. The individual elastic behaviors of elastin, collagen, and smooth muscle fibers are mathematically quantified. The hysteresis loop is characterized, in the time domain, by means of its viscous and inertial moduli; thus, the purely elastic behavior can be obtained. Finally, we suggest the possible constitutive mechanical equation of the aortic wall in conscious dogs and use this equation to show the individual contributions of the elastic, viscous, and inertial properties in the beat-to-beat hysteresis stress-strain relations.

Materials and Methods

Surgical Preparation

Fifteen male mongrel dogs aged 4.9±1.9 years and weighing 22.2±2.9 kg were prepared for the present study. On arrival at the animal facility, the dogs were vaccinated against common canine diseases and were treated for skin and intestinal parasites. For 20 days before surgery, they were appropriately fed and watered and assessed for adequate clinical status. The experiments were performed in accordance with the guiding principles of the American Physiological Society concerning the use of experimental animals.

Anesthesia was induced with intravenous thiopental sodium (20 mg/kg) and, after intubation, maintained with 2% enflurane carried in pure oxygen (4 L/min) through a Bain tube connected to a Bird Mark VIII respirator. A sterile thoracotomy was made at the left fifth intercostal space. A pressure microtransducer (Konigsberg P7, 1200-Hz frequency response) and a fluid-filled polyvinyl chloride catheter (outer diameter, 2.8 mm; for later calibration of the microtransducer) were implanted in the descending thoracic aorta through a stab wound in the left brachial artery. A pair of ultrasonic crystals (5 MHz, 4-mm diameter) was sutured onto the adventitia of the aorta, after minimal dissection, to measure external aortic diameter. The transit time of the ultrasonic signal (1580 m/s) was converted into distance by using a sonomicrometer (Triton Technology Inc, 100-Hz frequency response) and observed on the screen of an oscilloscope (Tektronix 465B) to confirm optimal signal quality. A polyvinyl chloride catheter (outer diameter, 2.3 mm) was advanced through the left mammary vein to lie in the superior vena cava or right atrium for drug administration. Two hydraulic cuff occluders made from silicon rubber were implanted around the descending thoracic aorta and inferior vena cava. The aortic cuff occluder was implanted at least 30 to 40 mm distal to the ultrasonic crystals to ensure that no artifacts appeared in diameter measurements during aortic occlusions. Before repairing the thoracotomy, all cables and catheters were tunneled subcutaneously to emerge at the interscapular space. All animals were allowed to recover under veterinary care. Ampicillin (20 $mg \cdot kg^{-1} \cdot d^{-1}$ per os) was given for 7 days after surgery. The catheters were flushed daily with heparinized saline.

Experimental Protocol

Experiments were performed starting on the seventh postoperative day. Each study was performed with the dog resting quietly on its right side in the conscious unsedated state.

The aortic pressure was measured with the pressure microtransducer, which had been calibrated against a Statham-P23 transducer connected to the aortic fluid-filled catheter. The zero reference point was set at the level of the right atrium. The Statham-P23 transducer had been previously calibrated with a mercury manometer. The external aortic diameter signal was calibrated in millimeters by using the step calibration facility of the sonomicrometer. Aortic pressure and diameter signals were stored on an FM tape recorder (Hewlett-Packard 3968-A) for later digital analysis, registered on a six-channel chart recorder (Gould 2600), and displayed on the screen of a four-channel monitor (Gould 51-2341). Instantaneous pressure-diameter loops were displayed on-line on a computer (PC-386) by using an analog-to-digital converter (National Instruments Lab PC). A specific program, developed in our laboratory,[16] was modified for this purpose.

Steady States

A 5% dextrose drip (0.25 mL/min) was started through the mammary vein catheter. At each steady state, the recordings of aortic pressure and external diameter were performed under the control condition and during phenylephrine administration (5 $\mu g \cdot kg^{-1} \cdot min^{-1}$) infused in parallel with the intravenous dextrose drip.

Assessment of Passive Elasticity

Recordings of aortic pressure and external diameter were made under basal steady state (PE_{basal}, where PE is passive elasticity) and during mechanical cuff occlusions of the descending aorta and vena cava (PE_{mech}). The occlusions were made to obtain a wide range of pressure-diameter relations. Also, aortic pressure and diameter were modified by means of intravenous bolus doses of angiotensin II (0.1 μg/kg) and nitroglycerin (25 mg/kg) to compare mechanical and pharmacological methods in the obtainment of changes in the aortic signals (PE_{angio} and PE_{nitro}, respectively). The assembly of PE_{angio} and PE_{nitro} data was called PE_{pharm}.

Assessment of VSM Elasticity

After PE recordings, VSM was activated by phenylephrine infusion. The instantaneous pressure-diameter loops were monitored until stabilization was achieved. We waited 15 to 20 minutes to ensure steady state under phenylephrine infusion and confirmed by visual inspection that the pressure-diameter

loops shifted toward a higher pressure level than that found in PE_{basal} and to the left of the PE_{mech} condition. Similar to PE recordings, aortic pressure and external diameter were recorded under basal steady state (SME_{basal}, where SME is smooth muscle elasticity) and during aortic and vena caval occlusions (SME_{mech}).

Two days later, the dogs were killed with an intravenous overdose of thiopental sodium followed by potassium chloride. The correct positioning of the dimension gauges in all dogs was verified at necropsy.

Data Collection

Aortic pressure and diameter signals were sampled and analyzed off-line on a Compaq Deskpro 25e computer equipped with a Data Translation 2801-A analog-to-digital converter. Sample frequency was set at 200 Hz. Approximately 20 consecutive beats during PE_{basal} and SME_{basal} conditions were averaged to obtain mean, systolic, diastolic, and pulse aortic pressures, diameter, and heart rate. The onset of diastolic aortic values was calculated as the point of maximum pressure occurring between the negative peak and the onset of the rapid upstroke of the first derivative of aortic pressure.

During the transient states (PE_{mech}, PE_{angio}, PE_{nitro}, PE_{pharm}, and SME_{mech}), all beats were digitized, starting from the beat before the onset of variation of the pressure and diameter signals until the beat before the maximal effect produced by the mechanical or pharmacological intervention.

Aortic wall thickness was calculated as the difference between the external aortic radius (r_e) and the internal aortic radius (r_i). To estimate r_i the following equation was used:

$$(1) \qquad r_i = \sqrt{r_e^2 - \frac{V}{\pi \cdot L}}$$

where V is the volume and L the length of a given aortic wall segment. This segment of thoracic descending aorta (25 to 30 mm) adjacent to the dimension gauges was marked with two sutures, and the distance between them was measured during surgery by using a caliper. After necropsy, this segment was carefully dissected free from surrounding tissue, cut at the markers, and weighed on a precision balance (Sartorius-Werke GMBH type 2442). The volume was calculated by using the weight of the aortic wall segment and assuming a tissue density of 1.066 g/mL. Since volume does not change in vivo, the values of r_i and aortic wall thickness could be calculated on a continuous basis.[17]

Strain (ε) was obtained from the ratio of midwall radius [$R=(r_e+r_i)/2$] to the nonstressed midwall radius (R_0) measured at ≈25 mm Hg of aortic pressure[17] during necropsy:

$$(2) \qquad \varepsilon = R/R_0$$

Stress (σ) and the incremental elastic modulus (E_{inc}) were assessed by using a linear elastic theory and assuming an isotropic homogeneous elastic material for the aortic wall.[18,19] E_{inc} was calculated as the slope of the stress-strain curve that theoretically describes the inherent stiffness of a vessel independent of its geometry:

$$(3) \qquad E_{inc} = 0.75\frac{d\sigma}{d\varepsilon}$$

$$(4) \qquad \sigma = \frac{2 \cdot P \cdot (r_e \cdot r_i)^2}{r_e^2 - r_i^2} \cdot \frac{1}{R^2}$$

where P is aortic pressure.

The computation of stress requires that opposing forces are at equilibrium. For this reason, we accepted this condition when the second derivative of strain was near zero, indicating the absence of acceleration.

It should be noted that the P, R, r_e, r_i, ε, and σ variables are functions of time and are incorporated into the equations developed in the "Appendix."

Constitutive Equation of the Aortic Wall

To obtain a complete mechanical characterization, we proposed a model to assess the elastic response of elastin (σ_E), collagen (σ_C), and smooth muscle (σ_{SM}) fibers and the viscous (σ_η) and inertial (σ_M) behavior of the aortic wall. This model assumes that total stress developed by the wall to resist stretching is governed by the following equations:

$$(5) \qquad \sigma = \sigma_E + \sigma_C + \sigma_{SM} + \sigma_\eta + \sigma_M$$

$$(6) \qquad \sigma = E_E \cdot (\varepsilon - \varepsilon_{0E}) + E_C \cdot f_C \cdot \varepsilon + E_{SM} \cdot f_A \cdot \varepsilon + \eta \cdot \frac{d\varepsilon}{dt} + M \cdot \frac{d^2\varepsilon}{dt^2}$$

where ε_{0E} is strain at zero stress, E_{SM} is the elastic modulus of the maximally contracted VSM, f_A is the activation function, η is the viscous modulus, and M is the inertial modulus. The first term in Equation 5 characterizes the linear elastic behavior of elastin fibers (see "Appendix," Equation 8). The second term represents the nonlinear behavior of collagen fibers (Equations 9 to 11). The first and second terms constitute the passive elastic stress-strain relation. The third term exists only under VSM activation and characterizes the elastic response of the VSM (Equations 12 to 16). The remaining terms represent the dynamic behavior of the aortic wall and are responsible for the hysteresis of the stress-strain relation (Equation 17).

Statistical Analysis

All measurements and calculated values were expressed as mean±SD. Linear regression was analyzed by the least-squares method. The presence of significant differences was assessed by paired *t* test or Tukey-B and Dunnett tests following ANOVA for repeated measures. Values of *t* and F ratio with $P<.05$ were considered statistically significant.[20] The nonlinear curve fittings were performed by using the Gauss-Newton iterative algorithm included in a scientific system (Asyst Software Technologies, Inc). To evaluate the curve fit performance, the normalized standard error of the estimate (NSE) was calculated in each animal according to the following expression:

$$(7) \qquad NSE = \frac{1}{\bar{\sigma}}\sqrt{\frac{\overline{\sigma - \hat{\sigma}}}{N - \gamma}}$$

where $\bar{\sigma}$ is the mean stress, $\hat{\sigma}$ is curve fit estimation of σ, N is the number of processed points, and γ is the number of constants involved in the corresponding equations (Equations 11 and 15).

Results

Steady State

Table 1 shows the hemodynamic parameters during control steady state and during steady state VSM activation by phenylephrine infusion. Heart rate was the only variable that presented no statistical differences with respect to the control condition.

Assessment of Viscous and Inertial Moduli (Hysteresis Characterization)

In Fig 1, top, recordings of pressure and diameter waveforms of the canine aorta are shown. Both signals present the same morphology, but the aortic diameter shows a time delay with respect to the aortic pressure. In Fig 1, bottom, the stress-strain hysteresis loop (open circles) calculated from these signals is plotted. A first approximation in the elimination of the hysteresis loop is shown when only the viscous stress has been subtracted (open squares). Once both viscous and inertial components have been removed, the actual stress-strain relation represents only the elastic properties of the aortic wall (filled circles). In the control condition, the viscous stress was 445±292% larger than inertial stress. Simi-

TABLE 1. Basal Hemodynamic State During Control Condition and Active Condition by Phenylephrine Infusion and Percent Changes With Respect to Control Condition

	Control (n=15)	Activation (n=8)	% Changes
Aortic systolic pressure, mm Hg	124.9±9.9	193.0±15.4*	52.1±12.7%
Aortic diastolic pressure, mm Hg	73.1±9.1	126.1±6.2*	72.9±20.7%
Aortic mean pressure, mm Hg	97.1±8.1	156.5±10.3*	60.5±14.9%
Aortic systolic diameter, mm	17.29±1.45	17.62±1.39†	1.74±1.71%
Aortic diastolic diameter, mm	15.54±1.41	16.37±1.28‡	4.63±3.60%
Aortic mean diameter, mm	16.52±1.40	17.07±1.33§	3.29±2.82%
Heart rate, bpm	112.7±19.5	104.3±23.8‖	−7.5±19.4%

bpm indicates beats per minute. Values are mean±SD.
*$P<.00001$, †$P<.02$, ‡$P<.005$, §$P<.01$, and ‖P=NS by paired t test with respect to the control condition in the eight dogs in which phenylephrine infusion was made.

larly, with phenylephrine infusion, the dynamic arterial wall behavior was mainly affected by the viscous properties yielding a viscous stress 453±141% larger than inertial stress. Both viscous and inertial moduli were significantly increased from the control state ($3.8\pm1.3\times10^4$ dyne $\cdot$ s $\cdot$ cm^{-2} and 61±42 dyne $\cdot$ s^2 $\cdot$ cm^{-2}) to the active state ($7.8\pm1.1\times10^4$ dyne $\cdot$ s $\cdot$ cm^{-2} [$P<.0005$] and 91±23 dyne $\cdot$ s^2 $\cdot$ cm^{-2} [$P<.05$]), respectively.

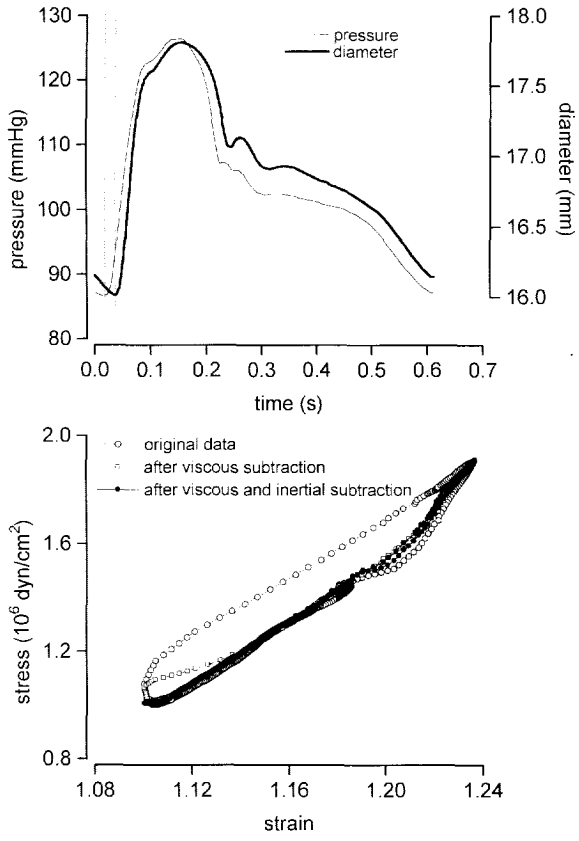

FIG 1. Top, Aortic diameter and pressure waveforms during control steady state. Arterial diameter shows a time lag due to viscous and inertial effects (vertical dashed lines). Bottom, Assessment of the purely elastic stress-strain relation. The aortic stress-strain relation (○) involves the elastic, viscous, and inertial properties conforming a hysteresis loop. By increasing values of the viscous modulus, the hysteresis area was reduced to a minimum (□). Ulterior increase of the inertial modulus produced the total disappearance of the hysteresis loop. The purely elastic stress-strain relation (●) is coincident with the stress-strain diastolic phase.

Transient State

Transient states were performed by using mechanical and pharmacological maneuvers producing marked variations in diameter and pressure waveforms (Fig 2, left). In Fig 2, right, the corresponding stress-strain relation obtained from the individual measured samples was depicted in the control condition and under phenylephrine administration. In the interval marked "diastole" (Fig 2, left), the second derivative of pressure (or stress) and diameter (or strain) is near zero, indicating the absence of acceleration and therefore the high degree of equilibrium required for the proper use of the stress-strain equations. In this interval, the purely elastic stress-strain curve was identified in the steady state.

Assessment of PE

During pharmacological maneuvers, systolic and diastolic pressures were respectively increased by 67±31% ($P<.0005$) (angiotensin bolus) and decreased by 35±23% ($P<.01$) (nitroglycerin bolus) with respect to the control steady state. Systolic and diastolic aortic diameters were respectively increased by 3.8±4.0% ($P<.025$) (angiotensin bolus) and decreased by 8.6±4.8% ($P<.01$) (nitroglycerin bolus) from the control steady state.

Mechanical interventions (descending thoracic aortic and vena caval occlusions) during the control condition increased systolic pressure (80±12% [$P<.00001$]) and decreased diastolic pressure (20±17% [$P<.0005$]) and increased systolic diameter (4±3% [$P<.0005$]) and decreased diastolic diameter (5±3% [$P<.00001$]) with respect to the basal steady state.

Descending thoracic aortic occlusion during phenylephrine infusion increased systolic pressure by 32±7% ($P<.00001$) from the steady state and increased systolic diameter by 2±0.5% ($P<.0005$) with respect to the activation steady state. Mechanical vena caval occlusion during phenylephrine infusion decreased both diastolic pressure by 33±17% ($P<.0005$) and diastolic diameter by 8±3% ($P<.00001$) with respect to the phenylephrine steady state. Fig 2, right, shows the stress-strain relations during control and activation conditions converted from pressure and diameter signals in a typical dog.

Elastic Behavior of the Elastin Fibers

Table 2 shows the totality of elastic parameters calculated from the whole population (15 dogs) assessed during PE_{mech} and compares these parameters with those obtained under PE_{angio}, PE_{nitro}, and PE_{pharm} in the dogs in which comparisons between occlusions and angiotensin

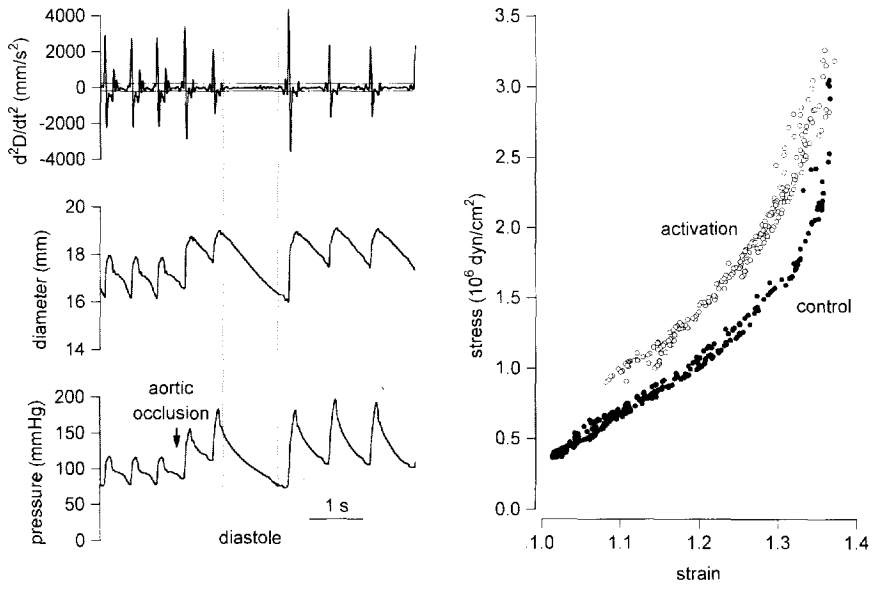

FIG 2. Left, Simultaneous recordings of the second derivative of aortic diameter (d^2D/dt^2, top), aortic diameter (middle), and aortic pressure (bottom) of beats during steady state, followed by descending thoracic aortic occlusion. The equilibrium conditions valid to calculate wall stress are reached when the d^2D/dt^2 is near zero or close to the noise level (horizontal solid lines, signal-to-noise relation, close to unity), indicating the absence of acceleration. This condition is sufficiently achieved during diastole, as can be seen in the recording of diameter and pressure. However, its application can be extended to the whole course of the heartbeat, extracting the few points placed beyond the threshold of the noise level. Right, Plot showing the stress-strain relations obtained by aortic occlusions in the control condition (●) and during vascular smooth muscle activation (○) in a typical dog.

and nitroglycerin bolus doses were performed. In all the studied parameters, no significant differences were found when ANOVA for repeated measures was made.

To find in which part of the cardiac cycle the break point of the stress-strain relation was placed, we performed comparisons between systolic, mean, diastolic, and maximum diastolic phase values of diameter, pressure, stress, and strain versus the break-point values in all dogs (Table 3). In this table, it can be observed that the level at which all parameters present no differences with respect to those corresponding to the break point is the maximum value assessed during the diastolic phase of the cycle.

The use of a linear mathematical model to characterize the elastic response of elastin fibers is supported by the highly linear correlation coefficients (0.972 ± 0.022 [$P<.0001$]) found in the analysis of the first portion of the stress-strain relations obtained with PE_{angio} (0.956 ± 0.045 [$P<.0001$]), PE_{nitro} (0.977 ± 0.023 [$P<.0001$]), PE_{pharm} (0.975 ± 0.023 [$P<.0001$]), and PE_{mech} (0.977 ± 0.031 [$P<.0001$]).

Elastic Behavior of Collagen Fibers (Assessment of Strain Recruitment Function)

The elastic modulus of the collagen fibers was $1102.5\pm532.2\times10^6$ dyne/cm^2. Fig 3 shows the nonlinear function representing the total aortic stress-strain relation and the corresponding linear function due to the elastic behavior of the elastin fibers (top left). Subtraction of both functions results in the collagen stress-strain relation (bottom left) of the entire population of dogs. Fig 3, top right, shows the mean values of measured and estimated (Equation 11) collagen stress-strain relations. The percentage of collagen fibers recruited from f_C (Equation 10) at each level of stretching is depicted in Fig 3, bottom right. It can be seen that the percentage of collagen fibers recruited at the deformation level observed at the break point of the stress-strain relation was $6.09\pm2.6\%$. The equation used to model the collagen stress response was successfully fitted in all dogs (NSE$=0.243\pm0.098$). The values of constants c_1, c_2, and c_3 obtained from the fit of the mean collagen stress-strain relation were 1.1452, 0.1117, and 0.0001, respectively (NSE$=0.188$).

Assessment of VSM Elasticity

Elastic behavior of smooth muscle fibers (assessment of activation function). Fig 4 shows the mean active stress-strain curves in control and VSM activation (top left) corresponding to eight dogs. Subtraction of stress values during the control condition from those obtained after excitation with phenylephrine results in the elastic behavior of the VSM (bottom left). As shown by these data, VSM exhibits a unimodal strain–active stress curve, with a maximum active stress of $0.949\pm0.57\times10^6$ dyne/cm^2 corresponding to a strain level of 1.299 ± 0.083.

TABLE 2. Elasticity Parameters During Control Condition Obtained From Mechanical Occlusions and Pharmacological Interventions

	PE_{mech} (n=15)	PE_{pharm} (n=7)	PE_{angio} (n=7)	PE_{nitro} (n=7)
E_E, 10^6 dyne/cm^2	5.02±1.48	4.94±1.98	5.44±1.86	4.87±1.88
σ_{BP}, 10^6 dyne/cm^2	1.357±0.294	1.449±0.447	1.524±0.464	1.402±0.355
ε_{BP}	1.231±0.085	1.250±0.075	1.258±0.088	1.248±0.067
P_{BP}, mm Hg	110.3±15.4	112.6±18.3	113.6±14.4	111.7±13.0
D_{BP}, mm	16.97±1.31	16.91±1.72	17.01±1.77	16.89±1.49
ε_{0E}	0.955±0.052	0.942±0.045	0.965±0.046	0.944±0.034

PE indicates passive elasticity; E_E, elastic modulus of elastin fibers; σ_{BP}, stress at break point; ε_{BP}, strain at break point; P_{BP}, aortic pressure at break point; D_{BP}, aortic diameter at break point; and ε_{0E}, strain at zero stress. Values are mean±SD. ANOVA for repeated measures (from seven dogs in which mechanical and pharmacological interventions were made) did not establish statistical differences between PE_{mech} (mechanical occlusions of descending thoracic aorta and vena cava), PE_{pharm} (pharmacological interventions, data from angiotensin and nitroglycerin bolus injections), PE_{angio} (angiotensin bolus), and PE_{nitro} (nitroglycerine bolus).

TABLE 3. Break Point Over the Cardiac Cycle

	Break Point Value	Diastolic Value	Mean Value	Systolic Value	Maximum Diastolic Part Value
σ, dyne/cm^2	1.357±0.294	0.775±0.255*	1.175±0.293*	1.636±0.337*	1.361±0.344‡
ε	1.231±0.085	1.120±0.078*	1.201±0.078*	1.264±0.082†	1.239±0.085‡
P, mm Hg	110.3±15.4	72.9±9.0*	97.0±8.1*	124.8±9.9*	107.1±9.4‡
D, mm	16.97±1.35	15.54±1.42*	16.52±1.41*	17.29±1.45†	16.98±1.43‡

σ indicates stress; ε, strain; P, aortic pressure; and D, aortic diameter. Values are mean±SD from all dogs (n=15).
*$P<.01$, †$P<.05$, and ‡P=NS by ANOVA for repeated measures and Dunnett's test with values at break point as control.

The maximum value of the VSM elastic modulus assessed by the maximum value of the derivative of the VSM stress-strain curve was $8.345\pm7.56\times10^6$ dyne/cm^2, occurring at a strain value of 1.283±0.079. Fig 4, top right, shows the mean values of measured and estimated (Equation 15) VSM stress-strain relations. The percent VSM activation function derived from Equation 16 is depicted in Fig 4, bottom right. The equation used to model the VSM muscle response was successfully fitted in all dogs (NSE=0.031±0.011). The values of constants m_1, m_2, m_3, m_4, and m_5 obtained from the fit of the mean VSM stress-strain relation were −71.23, 93.45, −0.49, 997.98, and 1.337, respectively (NSE=0.0125).

Constitutive Equation of the Aortic Wall

To reproduce the individual contribution of the elastic, viscous, and inertial behaviors to the total stress-strain relation, we applied the model proposed in Equation 6. Fig 5 depicts the elastic contribution of the passive components (elastin and collagen) to aortic stress-strain loops. These panels show that elastin fibers mainly govern the resistance to stretch. Fig 5 also shows the viscous and inertial components that are responsible for the hysteresis of the stress-strain loop. It can be seen that the wall viscosity is the most important dynamic contribution. Thus, the arterial wall is essentially viscoelastic in the beat-to-beat stress-strain relation, and the viscous effect can probably be attributed to smooth muscle in systole and the elastic effect to elastin fibers in diastole. In the control state, the VSM activation function is close to zero, since we assume that in this condition the VSM is not significantly activated; ie, it develops a small degree of activation whose elastic effects are negligible. Under activation of VSM (Fig 6), there was an increase in the collagen elastic contribution in the viscous stress and in the VSM elastic contribution. Similar to the previous case, the mechanical properties remain essentially viscoelastic. Fig 7 compares in a typical dog the measured and modeled (Equation 6) stress-strain relations and the stress time course during the control condition (top panels) and under activation (bottom panels), with the corresponding strain measured in each condition used as an input.

Discussion

The aim of the present study was to obtain a complete characterization of the arterial wall mechanics in conscious, unsedated, chronically instrumented dogs. In this work, a method to obtain this relation, called the constitutive equation,[11,12,14] was presented, and to our knowledge, no study regarding the complete specification of the mechanical properties of the aortic wall has previously been reported in conscious animals. To build the constitutive equation, we used second-order differential equations, where constant coefficients are the total elastic modulus, the viscous modulus, and the inertial modulus. The total elastic modulus was decomposed, quantifying the individual contributions to this modulus of the principal components of the arterial wall (elastin, collagen, and smooth muscle) and describing them by a mechanical model. The viscous and inertial moduli were assessed by using the criterion of disappearance of the hysteresis loop to obtain the purely elastic behavior. Finally, the individual contributions of the elastic, vis-

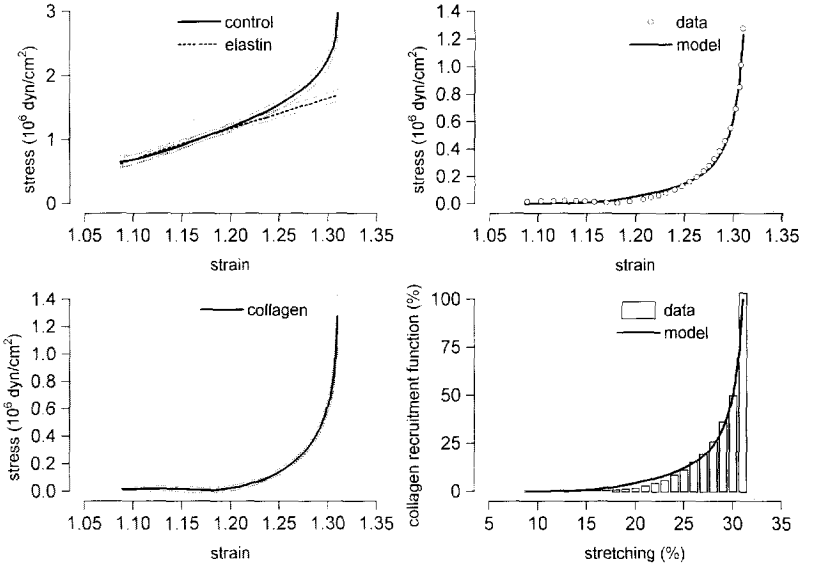

FIG 3. Graphic determination of collagen fiber elasticity. Top left, Nonlinear function depicted on the graph is the entire stress-strain relation during the control condition, and the linear function is the elastic behavior of the elastin fibers. Bottom left, Points obtained by subtracting values of the linear function from the control stress-strain relation at any value of strain determine a new function, representing the collagen stress-strain relation. Both panels show the mean stress-strain relations and their respective SEM in stress over all the range of strain (thin dotted lines). Top right, Mean collagen stress-strain relation (○) is shown. The nonlinear function (solid line) is the output of Equation 11 used to model the collagen response whose constants were assessed by nonlinear curve fit. Bottom right, Percent recruitment of collagen fibers was calculated by the recruitment function (Equation 10) at each level of stretching.

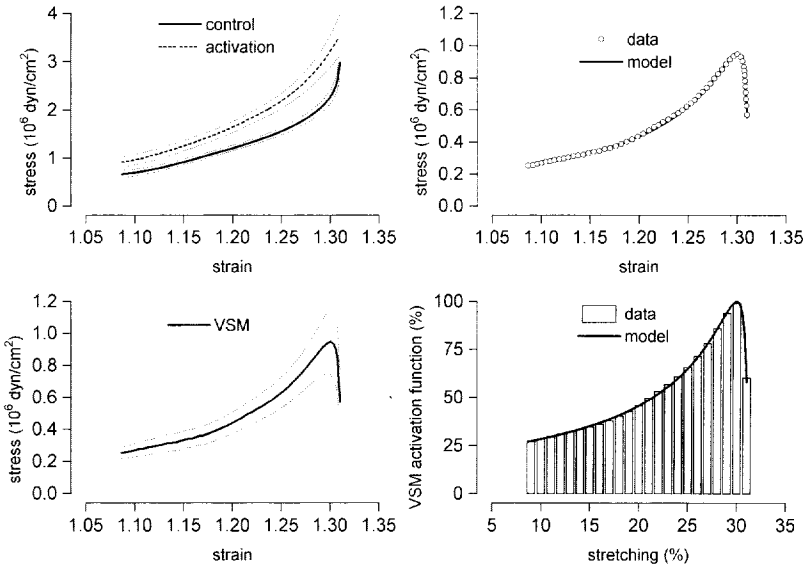

FIG 4. Graphic determination of smooth muscle fiber elasticity. Top left, Graph showing the total stress-strain relation during the control condition and during activation of vascular smooth muscle (VSM). Bottom left, Points obtained by subtracting values of the control condition from the stress values under activation of VSM at any value of strain determine a new function, representing the stress exerted by the active smooth muscle. Both panels show the mean stress-strain relations and their respective SEM in stress over all the range of strain (thin dotted lines). Top right, Mean smooth muscle stress-strain relation (○). The nonlinear function (solid line) is the output of Equation 15 used to model the smooth muscle response whose constants were assessed by nonlinear curve fit. Bottom right, The VSM activation function as a function of percent stretching from the unstressed values representing the level of activation at each step of arterial deformation.

cous, and inertial properties to the hysteresis loop could be achieved with the methods presented in the present study.

The instrumentation techniques used to obtain the pressure-diameter relation in the conscious animal[18] have been reproduced in our laboratory,[6-9] allowing accurate and reproducible measurements.[10,21]

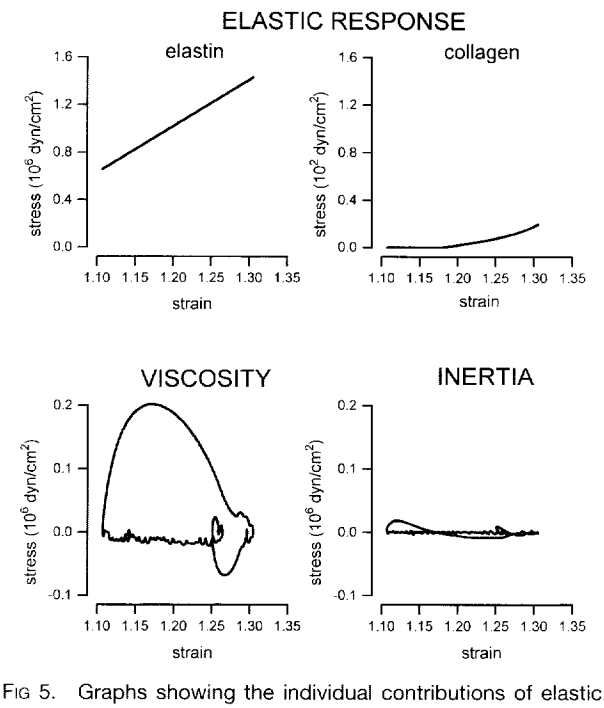

FIG 5. Graphs showing the individual contributions of elastic, viscous, and inertial properties to the beat-to-beat aortic wall behavior obtained from the model (Equation 6). In control steady state, the activation function is close to zero; thus, the passive resistance to stretch is mainly supported by the elastin fibers because of the incipient contribution of collagen fibers. The viscous behavior is responsible for the hysteresis of the loop, since the inertial stress-strain relation is close to zero. Thus, the arterial wall is essentially viscoelastic. The viscous effect can probably be attributed to smooth muscle and is mainly developed during systole; the elastic effect, to elastin fibers being predominant during diastole.

Aortic signals were converted into stress and strain by using a thick-walled cylindrical tube model and linear elastic theory.[18] Stress was calculated instantaneously in the overall cardiac cycle, considering the nonvariability of wall volume segments.[17] Even though it might appear that the condition of equilibrium was absent, the analysis of pressure-diameter relations shows that most of the sampled data corresponded to the diastolic phase of the cardiac cycle (Fig 1). In this phase, the second derivative of diameter (or strain) was near zero, indicating the absence of acceleration and therefore a high degree of equilibrium. This fact could have been a major limitation in this approach, since we needed the instantaneous beat-to-beat stress-strain relation to apply the procedure that gives the purely elastic behavior. To overcome this problem, we defined a threshold in the second derivative of diameter, below which we assumed that it was impossible to separate signal from noise. The points beyond this threshold were withdrawn from the stress-strain relation (Fig 2). In all cases, only few points were found in this condition because of the chosen acquisition sample rate.

The first step in the present study was the evaluation of the system parameters (coefficients of the second-order equation), and the second step was the use of these parameters to predict the behavior of the system.[22] In the present work, it was possible to assess the purely elastic aortic behavior in conscious dogs. This behavior was close to the diastolic stress-strain relation, demonstrating that during this phase of the beat, the very low harmonic contents yield a negligible viscous-inertial behavior. However, the diastolic phase represents only half of the cardiac cycle, whereas our procedure involves all the cardiac cycle in the assessment of the purely elastic stress-strain relation. With the same procedure, it was possible to quantify the inertial and viscous moduli. In the descending thoracic aorta, the inertial modulus was negligible compared with the viscous and elastic behaviors, in agreement with Peterson et al,[23] who stated that the behavior of arteries was mainly viscoelastic. Our results showed a mean viscous modulus of $3.8 \pm 1.3 \times 10^4$ dyne · s · cm^{-2} and a mean elastic modulus of $4.99 \pm 1.58 \times 10^6$ dyne/

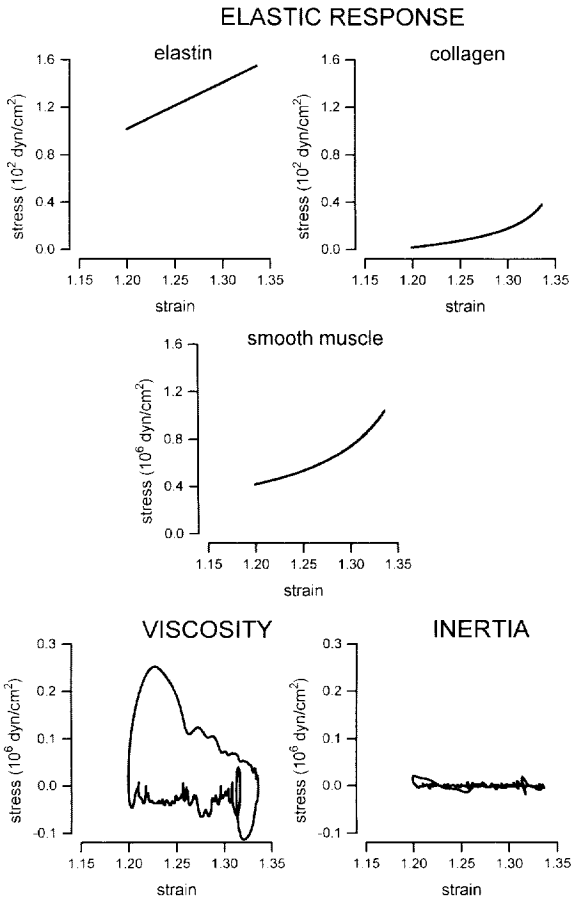

FIG 6. Graphs showing the individual contributions of elastic, viscous, and inertial properties to the beat-to-beat aortic wall behavior under activation obtained from the model (Equation 6). In contrast to the control condition, the passive resistance to stretch is mainly supported by elastin fibers as well as by the activated vascular smooth muscle (VSM). Similar to behavior in the control state, the viscous behavior is responsible for the hysteresis of the loop and is mainly developed during systole. The inertial stress-strain relation is close to zero, indicating that also under activation, the wall viscosity is the most important dynamic contribution and the arterial wall is essentially viscoelastic.

cm^2 in the control condition. From the data reported by Peterson et al in thoracic aorta, we calculated a mean viscous modulus of 22 ± 10^4 dyne · s · cm^{-2} and a mean elastic modulus of 5.3×10^6 dyne/cm^2, suggesting an understimation in our calculated viscous modulus, whereas the elastic modulus is very similar to their results. A possible explanation could be that the different experimental conditions and technology used by these authors in the pressure-diameter measurements could have altered the real time lag between signals, thereby increasing viscocity.

In the beat-to-beat steady state, the elastic deformation is proportional to the potential energy stored during systole that will be yielded to the system during diastole, whereas the viscous loop (Figs 5 and 6) quantifies the absorption of energy by the vessel wall. The increment of the viscous modulus under activation signifies that this coefficient is dependent on pressure and on the level of smooth muscle activation, material responsible for the viscous behavior of the aortic wall. The viscous loss of energy is small, but it is an interesting aspect of hemodynamics that has been little explored.[13] The larger viscous modulus when the muscle is active indicates a greater expenditure of energy in the pulsatile expansion of the vessel with each heartbeat.[10]

Rigorously speaking, the inertial modulus is a proportionality constant between force and the acceleration developed by a given material and quantifies the resistance to acceleration presented by the body. In systemic arterial wall dynamics, inertial forces might develop at the beginning of systole concomitant with the very fast increase in diameter.[12] In our case and in agreement with Peterson et al,[23] the inertial term is negligible in the relation between stress and strain in the arterial wall under physiological conditions; ie, the inertial stress is too small to influence the stress-strain loop (Figs 5 and 6), indicating that the artery is essentially viscoelastic. During phenylephrine administration, the inertial modulus was increased with respect to the control condition. This result implies that (according to the use of mass as a quantitative measure of inertia) the aortic wall mass, defined as the addition of the individual mass of each structural constituent, should also be increased under activation. It is obvious that factors other than the wall mass should offset the magnitude of the inertial modu-

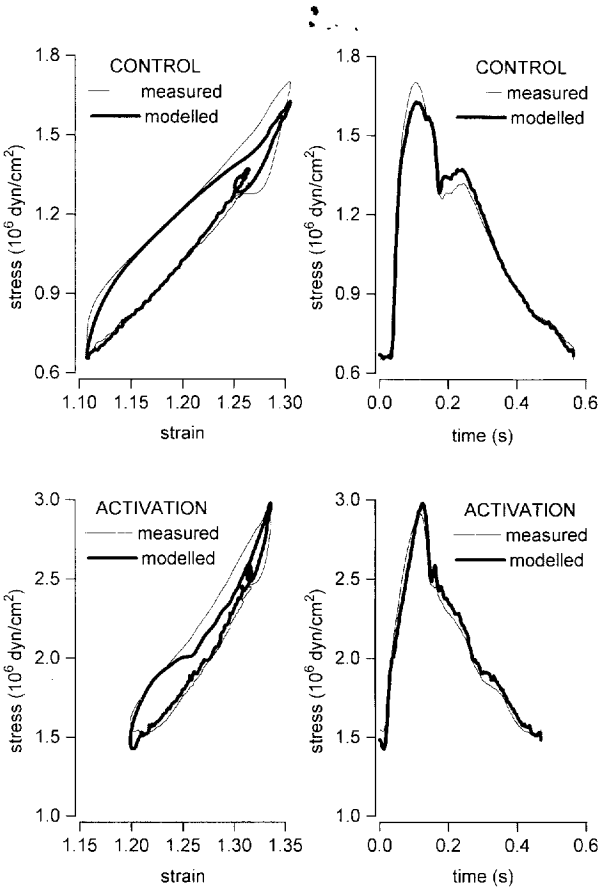

FIG 7. Top, Comparison between measured and modeled stress-strain relations (left) and stress waveforms (right) using as input the corresponding measured strain in a typical dog in the control condition. The hysteresis involved in the estimated stress-strain relations were lower than the measured ones. Bottom, Comparison between measured and modeled stress-strain relations (left) and stress waveforms (right) using as input the corresponding measured strain in a typical dog under phenylephrine administration. In this case, it was also found that the hysteresis involved in the estimated stress-strain relations were lower than the measured ones, and because of the activated VSM, the differences were more pronounced.

lus. This modulus can be codetermined by the level of aortic pressure and/or the stiffness of the aortic wall, because at greater pulse pressures, marked nonlinearity of the inertial behavior can occur.[12] Among the possible factors producing nonlinear inertial behavior, frequency could play an important role, as was reported for the viscous modulus of the arterial wall.[24] In this case, the inertial modulus must be regarded as a mathematical abstraction that mimics the inertial behavior of the aortic wall and not as a physical constant. Other effects such as the radial acceleration of blood could influence this phenomenon, and for these reasons, further studies would be necessary to evaluate whether the alterations that could be found in the inertial modulus under different physiopathological states were due exclusively to intrinsic changes in the arterial wall.

There are two theories that explain the viscosity of the vessel. Passive theories assume that viscosity is simply a property of the aortic wall constituents, and it is generally assumed that the vascular smooth muscle is mainly responsible for this behavior.[25,26] Bulbring et al[27] have shown that viscosity is greater in muscular than in elastic arteries, suggesting that this point of view is possible. The location of viscous elements in the infrastructure of the muscle cell has not been identified. Among several possibilities, it has been suggested that viscosity could be ascribed to (1) the protoplasm itself, (2) the viscous resistance of the cell matrix encountered by the sliding of actin and myosin filaments during muscle contraction, and finally (3) the cell membrane that could act as a restraint presenting a viscoelastic nature.[10] These explanations must be taken carefully, since some stretch relaxation was still observed when the muscle was inactivated by prolonged immersion in calcium-free solutions or iodoacetic acid,[13,28] suggesting that smooth muscle cannot be the only source of these effects. This observation could be a possible limitation in the present model because collagen, elastic, and ground substance might also present viscous behavior. In collagen fibers, both elasticity and viscosity probably depend to some extent on the orientation of the fibers.[29] Another theory (active theory) to explain the cause of hysteresis takes into account the force-generating mechanism of the muscle[30] as well as the myogenic response to stretching.[10,31,32] These possible explanations are not mutually exclusive, and hysteresis might be the result of several factors. Viscous behavior may affect the velocity of the pulse wave. Any system that presents elastic and viscous behavior acts on the size and shape as well as the velocity of the wave. For these reasons, the pulse-wave velocity measured in clinical practice must be carried out by identifying the points next to the foot of the wave where the effects of viscosity and the reflected wave are negligible.[33]

In brief, VSM exhibits two kinds of response: one represented by the viscous behavior present in the beat-to-beat steady state, which affects mainly the systolic stress-strain relation, and the other related to pharmocological activation, which can modify the elastic behavior of the muscle through the elastic contribution of the contracted muscle.

The elastic modulus of elastin fibers and the coordinates of the break point are the result of the arterial wall structure and for this reason can be evaluated by mechanical or pharmacological maneuvers. The diameter and pressure values at the break point did not change with the different maneuvers, since the rapid variations in the stress-strain relations reflect solely the intrinsic properties of the aortic wall.

We found that the break point was close to the maximum diastolic value and that this might represent the value at which the reflected wave reaches its maximum. Beyond this point until the onset of the next beat, the stress-strain relation reflects the purely elastic behavior of the aortic wall. This suggests that the mean diastolic pressure used by O'Rourke et al[34] as an index of coronary perfusion is determined exclusively by the elastic components and not by the transient effect of viscosity and inertia, which depends mainly on heart rate. Beyond the break point, collagen participation is increased, and at high levels of deformation, the totality of the collagen fibers resists stretching. Thus, the hysteresis loop is diminished because of the double effect of a collagen predominance and a decrease in heart rate produced by the high pressure level. In contrast, below the break point, the viscous behavior is predominantly accounted for by smooth muscle cells.

The recruitment of collagen fibers as a function of deformation showed that with a 30% stretching of the arterial wall with respect to the unstressed diameter, 100% of the collagen fibers resisted deformation, whereas at the break point (23% of deformation with respect to the unstressed diameter), only 6% of the total collagen fibers was recruited (Fig 3, bottom right). The recruited collagen fibers were increased from 6% to 100% with only a 7% increase in deformation (from 23% to 30%), evidencing their highly nonlineal behavior. Thus, in control conditions the nonlinearity of the stress-strain relation is due exclusively to the collagen recruitment function. To model this function, we used a trigonometric tangent function used by others with excellent results.[35,36]

The VSM activation function depends on the degree of smooth muscle activation. We assumed that under phenylephrine administration the smooth muscle is maximally contracted and thus the term E_{SM} represents the maximum value of the VSM elastic modulus. This skewed function was represented as a function of the percent deformation from the unstressed values and represents the level of activation at each step of arterial deformation. Fig 4, bottom right, shows that its maximum value corresponded to 28% of stretching and that beyond this point, stress fell abruptly. This curve does not reflect the exact overlapping of actin-myosin bridges because the series arrangement of the series elastic component and the contractile element transforms a symmetric curve into a skewed one. For this reason, we used a modified lorentzian function with five constants with excellent curve fit performance.

We identified the constants of the constitutive equation for the aortic wall (Equation 6) in conscious dogs by using the individual characterization of its structural constituents and exploring their contribution to stress. The stress-strain relations estimated with Equation 6 in control resting conditions and under activation of the smooth muscle were similar to the respective measured ones. In both cases, the hysteresis involved in the estimated stress-strain relations were lower than the measured ones. These differences were found at the highest level of stress and strain near the systolic point. At this stage, it is possible that the hysteresis of the aortic wall is complicated by the myogenic response,[10,31,32] consisting of a small rapid stretching of the

vessel immediately followed by an active contraction of the muscle. However, to our knowledge, no study regarding this effect in the aortic wall has been reported.

Characterization of the mechanical properties of the individual structural constituents could provide insight into the physiological and pathological processes that can affect the arterial wall, such as hypertension, atherosclerosis, aging, and diabetes.[37] With this approach, it would be possible to know the consequences of structural alterations of the arterial wall, and by assessing its individual mechanical behaviors before and after treatment, it could be determined whether these alterations could be reversed.

In conclusion, the accurate assessment of the mechanical properties of the individual components of the aortic wall in conscious dogs allows the construction of a possible constitutive equation. The purely elastic stress-strain relation can be obtained by extracting the viscous and inertial arterial behaviors; thus, the arterial wall can be characterized on the basis of three different hookean materials (E_E, E_C, and E_{SM}, with the latter only under activation) and two nonlinear functions, f_A and f_C. Finally, we suggest that another pathway (probably the myogenic response of vascular smooth muscle) in addition to the passive viscosity of the smooth muscle might play a role in the hysteresis of the stress-strain loop.

Appendix

Elastic Modulus of Elastin Fibers (E_E)

The first part of the stress-strain relation shows a linear behavior. Beyond a certain value of stress, the "break point," the relation curves upward as collagen fibers are recruited.[7,8] Up to this critical point, the linear response of the aortic wall can be fitted with a linear model where E_E is the slope of the linear relation. Therefore, the stress-strain relation for this linear portion can be written as follows:

$$\sigma_E = E_E \cdot (\varepsilon - \varepsilon_{0E}) \tag{8}$$

where E_E expresses the elastic modulus of elastin fibers, and ε_{0E} is the strain-axis intercept.

Elastic Modulus of Collagen Fibers (E_C)

To describe the elastic response of collagen fibers, it is necessary to separate the stress-strain relation corresponding to elastin from the overall stress-strain relation. According to this approach, the collagen behavior is given by the following relation:

$$\sigma_C = \sigma - \sigma_E = E_C \cdot f_C \cdot \varepsilon \tag{9}$$

where E_C expresses the elastic modulus of collagen fibers. To obtain E_C, it is necessary to calculate the difference between the values of the measured stress-strain relation and those obtained using Equation 8 at each strain value.

Recruitment Function of Collagen Fibers as a Function of Strain (f_C)

To model the collagen elastic response represented by the stress developed by collagen fibers resisting stretch, we multiplied the elastic modulus of the collagen fibers, E_C, by a normalized morphology function named the strain recruitment function, f_C, expressed as follows:

$$f_C = c_1 \cdot \tan\left(\frac{\varepsilon - c_2}{c_3}\right) \tag{10}$$

where c_1, c_2, and c_3 are three constants assessed by nonlinear curve fitting. Then, substituting Equation 10 into Equation 9 gives the following:

$$\sigma_C = E_C \cdot f_C \cdot \varepsilon = E_C \cdot c_1 \cdot \tan\left(\frac{\varepsilon - c_2}{c_3}\right) \cdot \varepsilon \tag{11}$$

Mechanics of VSM

To describe the mechanics of VSM, a modified three-element Maxwell model was used.[9] According to this model, total stress can be written as follows:

$$\sigma = E_E \cdot (\varepsilon - \varepsilon_{0E}) + E_C \cdot f_C \cdot \varepsilon + \sigma_{SM} \tag{12}$$

where σ_{SM} is the active stress supported by the assembly of an elastic spring coupled in series with the contractile element (CE-SEC). The passive stress developed by the parallel elastic component (σ_{PE}) could be evaluated by using the elastic passive behavior of elastin (Equation 8) and collagen (Equation 9) obtained during control conditions:

$$\sigma_{PE} = E_E \cdot (\varepsilon - \varepsilon_{0E}) + E_C \cdot f_C \cdot \varepsilon \tag{13}$$

Thus, the computation of active stress supported by the assembly of CE-SEC was made by subtracting the aortic stress-strain relation in the control condition from the aortic stress-strain relation obtained under phenylephrine administration at the same level of strain:

$$\sigma_{SM} = \sigma - \sigma_{PE} \tag{14}$$

Assessment of Activation Function as a Function of Strain (f_A)

The smooth muscle active stress-strain relation obtained from in vitro studies has been characterized in several works.[38-40] Recently, this was obtained in conscious animals: the smooth muscle elastic modulus versus strain was shown as a skewed unimodal curve with a maximum value (E_{SM}) that represents the highest level of elasticity that can be reached for this level of activation.[9] To model the smooth muscle active stress-strain relation, we proposed the following skewed function composed by a modified lorentzian function multiplied by the maximum value of the smooth muscle modulus, E_{SM}:

$$\sigma_{SM} = E_{SM} \cdot f_A \cdot \varepsilon = E_{SM} \cdot \frac{m_1 \cdot \varepsilon + m_2}{m_3 + m_4 \cdot (\varepsilon - m_5)^2} \cdot \varepsilon \tag{15}$$

where m_1, m_2, m_3, m_4, and m_5 are the constants assessed by nonlinear curve fitting, E_{SM} is the maximum value of the elastic modulus of the VSM, and f_A is the activation function characterized as follows:

$$f_A = \frac{m_1 \cdot \varepsilon + m_2}{m_3 + m_4 \cdot (\varepsilon - m_5)^2} \tag{16}$$

Assessment of the Purely Elastic Stress-Strain Relation

The total stress generated by the wall to oppose stretching is commonly attributed to the combined effects of wall elasticity, wall viscosity, and inertia. Bauer and colleagues[11,12] have developed a procedure that subdivides the wall stress into three terms, the first of which depends on ε, the second on the first derivative of ε (velocity), and the third on the second derivative of ε (acceleration):

$$\sigma = E \cdot \varepsilon + \eta \cdot \frac{d\varepsilon}{dt} + M \frac{d^2\varepsilon}{dt^2} = \sigma_{elastic} + \sigma_{viscous} + \sigma_{inertial} \tag{17}$$

where E, η, and M are the elastic, viscous, and inertial moduli. The first term is the elastic stress; the second, the viscous stress; and the last, the inertial stress. By definition, the purely elastic stress-strain relation courses along the same curve for increasing and decreasing radius; therefore, in this diagram no hysteresis loop appears. To separate the purely elastic wall properties, one must subtract the viscous and the inertial stress from the total aortic stress, finding the optimal value through the criterion of disappearance of the hysteresis loop. The input for Equation 17 was ε. In a first step, M was considered to be equal

to zero, and increasing values of η were given by analyzing by visual inspection the reduction of the hysteresis loop area. When the area reached a minimum (considered to be the value that maintained the clockwise course of the loop), M values were incremented in steps to obtain the total disappearance of the hysteresis loop. Units used were dynes, centimeters, and seconds.

Acknowledgment

The authors wish to thank Elena Lascano, BSc, for her help in the revision of the manuscript.

References

1. Nichols WW, O'Rourke MF, Avolio AP, Yaginuma T, Murgo JP, Pepine CJ, Conti CR. Age-related changes in left ventricular/arterial coupling. In: Yin FCP, ed. *Ventricular Vascular Coupling: Clinical, Physiological, and Engineering Aspects*. New York, NY: Springer-Verlag; 1987:79-114.
2. Fitchett DH. LV-arterial coupling: interactive model to predict effect of wave reflections on LV energetics. *Am J Physiol*. 1991; 261:H1026-H1033.
3. Simon A, Levenson J. Overview on atherosclerotic systolic hypertension. *Int J Cardiol*. 1987;16:1-18.
4. Simon AC, O'Rourke MF, Levenson J. Arterial distensibility and its effects on wave reflection and cardiac loading in cardiovascular disease. *Coron Artery Dis*. 1991;2:1111-1120.
5. Clark JM, Glagov S. Transmural organization of the arterial media: the lamellar unit revisited. *Arteriosclerosis*. 1985;5:19-34.
6. Cabrera Fischer EI, Armentano RL, Levenson J, Barra JG, Morales MC, Breitbart GJ, Pichel RH, Simon AC. Paradoxically decreased aortic wall stiffness in response to vitamin D_3–induced calcinosis: a biphasic analysis of segmental elastic properties in conscious dogs. *Circ Res*. 1991;68:1549-1559.
7. Cabrera Fischer EI, Levenson J, Barra JG, Armentano RL, Pichel RH, Simon AC. Preventive effect of chronic converting enzyme inhibition on aortic stiffening induced by renovascular hypertension in conscious dogs. *Cardiovasc Res*. 1993;27:1039-1044.
8. Armentano RL, Levenson J, Barra JG, Cabrera Fischer EI, Breitbart GJ, Pichel RH, Simon A. Assessment of elastin and collagen contribution to aortic elasticity in conscious dogs. *Am J Physiol*. 1991;260:H1870-H1877.
9. Barra JG, Armentano RL, Levenson J, Cabrera Fischer EI, Pichel RH, Simon A. Assessment of smooth muscle contribution to descending thoracic aortic elastic mechanics in conscious dogs. *Circ Res*. 1993;73:1040-1050.
10. Milnor WK. *Hemodynamics*. Baltimore, Md: Williams & Wilkins Co; 1982:56-96.
11. Bauer RD, Busse R, Schabert A, Summa Y, Wetterer E. Separate determination of the pulsatile elastic and viscous forces developed in the arterial wall in vivo. *Pflugers Arch*. 1979;380:221-226.
12. Bauer RD. Rheological approaches of arteries. *Biorheology*. 1984; 1(suppl):159-167.
13. Lundholm L, Mohme-Lundholm E. Length at inactivated contractile elements, length-tension diagram, active state and tone of vascular smooth muscle. *Acta Physiol Scand*. 1966;68:347-359.
14. Fung YC. *Biomechanics*. New York, NY: Springer-Verlag; 1981.
15. Dobrin PB. Mechanical behaviour of vascular smooth muscle in cylindrical segments of arteries in vitro. *Ann Biomed Eng*. 1984;12:497-510.
16. De Forteza E, Armentano RL, Biagetti M, Rodríguez Chatruc EM. Real-time pressure-volume diagrams for the evaluation of ventricular function. *J Biomed Eng*. 1986;8:200-205.
17. Dobrin PB, Rovick AA. Influence of vascular smooth muscle on contractile mechanics and elasticity of arteries. *Am J Physiol*. 1969;217:1644-1652.
18. Pagani M, Mirsky I, Biag H, Manders WT, Kerkhof P, Vatner SF. Effects of age on aortic pressure-diameter and elastic stiffness-stress relationships in unanesthetized sheep. *Circ Res*. 1979;44:420-429.
19. Vatner SF, Pasipoularides A, Mirsky I. Measurement of arterial pressure-dimension relationships in conscious animals. *Ann Biomed Eng*. 1984;12:521-534.
20. Winer BJ. *Statistical Principles in Experimental Design*. New York, NY: McGraw-Hill Book Co; 1962:4-148.
21. Nichols WW, O'Rourke MF. *McDonald's Blood Flow in Arteries*. London, England: Edward Arnold Publishers, Ltd; 1990.
22. Cobelli C, Carson ER, Finkelstein L, Leaning MS. Validation of simple and complex models in physiology and medicine. *Am J Physiol*. 1984;246:R259-R266.
23. Peterson LH, Jensen RE, Parnell J. Mechanical properties of arteries in vivo. *Circ Res*. 1960;8:622-639.
24. McDonald DA. *Blood Flow in Arteries*. Baltimore, Md: Williams & Wilkins Co; 1974:238-419.
25. Bozler E. An analysis of the properties of smooth muscle. *Cold Spring Harb Symp Quant Biol*. 1936;4:260-266.
26. Stacy RW, Williams DT, Worden RD, McMorris RO. *Essentials of Biological and Medical Physics*. New York, NY: McGraw-Hill Publishing Co; 1955.
27. Bulbring E, Brading AF, Jones AW, Tomita T. *Smooth Muscle*. Baltimore, Md: Williams & Wilkins Co; 1970.
28. Axelsson J. Mechanical properties of smooth muscle, and the relationship between mechanical and electrical activity. In: Bulbring E, Brading AF, Jones AW, Tomita T, eds. *Smooth Muscle*. Baltimore, Md: Williams & Wilkins Co; 1970:289-315.
29. Stromberg DD, Wiederhielm CA. Viscoelastic description of a collagenous tissue in simple elongation. *J Appl Physiol*. 1969;26:857-862.
30. Ruegg MD. Smooth muscle tone. *Physiol Rev*. 1971;51:201-247.
31. Bayliss WM. On the local reactions of the arterial wall to changes in internal pressure. *J Physiol (Lond)*. 1902;28:220-231.
32. Spark HV. Effect of quick stretch on isolated vascular smooth muscle. *Circ Res*. 1964;15(suppl I):I-1254-I-1260.
33. Armentano RL, Simon A, Levenson J, Chau NP, Megnien JL, Pichel RH. Mechanical pressure versus intrinsic effects of hypertension on large arteries in humans. *Hypertension*. 1991;18:657-664.
34. O'Rourke MF, Avolio AP, Nichols WW. Left ventricular-systemic arterial coupling in humans and strategies to improve coupling in disease states. In: Yin FCP, ed. *Ventricular Vascular Coupling: Clinical, Physiological, and Engineering Aspects*. New York, NY: Springer-Verlag; 1987:1-19.
35. Tardy Y, Meister JJ, Perret F, Brunner HR, Arditi M. Non-invasive estimate of the mechanical properties of peripheral arteries from ultrasonic and photoplethysmographic measurements. *Clin Phys Physiol Meas*. 1991;12:39-54.
36. Langewouters GJ, Wesseling KH, Goedhard WJ. The static elastic properties of 45 human thoracic and 20 abdominal aortas in vitro and the parameters of a new model. *J Biomech*. 1984;17:425-435.
37. Yin FCP, Ting CT. Compliance changes in physiological and pathological states. *J Hypertens*. 1992;10(suppl 6):S31-S33.
38. Cox RH. Arterial wall mechanics and composition and the effects of smooth muscle activation. *Am J Physiol*. 1975;229:807-812.
39. Cox RH. Effects of norepinephrine on mechanics of arteries in vitro. *Am J Physiol*. 1976;231:420-425.
40. Murphy RA. Mechanics of vascular smooth muscle. In: Bohr DF, Somlyo AP, Sparks HV Jr, eds. *Handbook of Physiology, Section 2: The Cardiovascular System, Volume II*. Bethesda, Md: American Physiological Society; 1980:325-351.